DOI:10.1158/1078-0432.CCR-05-0627

Clinical Cancer Research

Antitumor Efficacy of Capecitabine and Celecoxib in Irradiated and Lead-Shielded, Contralateral Human BxPC-3 Pancreatic Cancer Xenografts: Clinical Implications of Abscopal Effects

Carmelo Blanquicett, M. Wasif Saif, Donald J. Buchsbaum, et al.

Clin Cancer Res 2005;11:8773-8781. Published online December 16, 2005.

DOI:10.1158/1078-0432.CCR-05-0627

Antitumor Efficacy of Capecitabine and Celecoxib in Irradiated and Lead-Shielded, Contralateral Human BxPC-3 Pancreatic Cancer Xenografts: Clinical Implications of Abscopal Effects

Carmelo Blanquicett,[1,5] M. Wasif Saif,[5] Donald J. Buchsbaum,[4,5] Mohamad Eloubeidi,[2] Selwyn M. Vickers,[2,5] David C. Chhieng,[3] Mark D. Carpenter,[5] Jeffrey C. Sellers,[4,5] Suzanne Russo,[4,5] Robert B. Diasio,[1,5] and Martin R. Johnson[1,5]

Abstract

Purpose: X-ray therapy (XRT) remains one of the major modalities used to treat patients diagnosed with locally advanced pancreatic adenocarcinoma. However, the effect of XRT on metastatic tumors outside the field of irradiation (abscopal effect) remains largely unknown. In the current study, we examined the effect of XRT alone and in combination with capecitabine and/or celecoxib in both irradiated and lead-shielded contralateral BxPC-3 pancreatic cancer xenografts. This chemoradiation regimen was chosen based on our molecular analysis of pancreatic adenocarcinoma.

Experimental Design: Athymic mice were injected bilaterally with BxPC-3 cells and treatment was initiated 28 days postimplant. During XRT (2 Gy for 5 consecutive days, administered on days 0 and 24), one flank was irradiated whereas the rest of the body (including the contralateral tumor) was lead shielded. Capecitabine (350 mg/kg) was administered on days 0 to 13 and 24 to 37. Celecoxib was initiated in the diet at 100 ppm (equivalent to 20 mg/kg/d p.o.) and administered throughout the study.

Results: In irradiated xenografts, capecitabine and XRT showed synergistic anitiumor efficacy ($P = 0.008$), which was further improved with the addition of celecoxib ($P < 0.001$). In contralateral shielded xenografts, abscopal effects were observed. Whereas monotherapy with XRT showed significant reduction in tumor area in irradiated xenografts, growth was promoted by 23% ($P < 0.001$) in contralateral lead-shielded tumors in the same animals relative to untreated tumors. Interestingly, synergistic antiproliferative efficacy occurred in these contralateral tumors when capecitabine was administered ($P < 0.001$), despite being outside the irradiated field. The addition of celecoxib further inhibited tumor growth ($P < 0.001$). This trimodal combination most effectively stabilized disease in both shielded and irradiated tumors; however, tumor eradication was not observed. There were no significant changes in thymidine phosphorylase, dihydropyrimidine dehydrogenase, or cyclooxygenase-2 mRNA levels in irradiated or lead-shielded tumors, suggesting that efficacy cannot be predicted solely from these previously identified indicators of response. Immunohistochemistry examining the proliferation marker Ki-67 showed concordance with tumor response in both irradiated and contralateral shielded xenografts.

Conclusions: These results have implications in the rational design of treatment paradigms for pancreatic cancer where metastatic disease remains the primary cause of patient morbidity and abscopal effects in tumors outside the field of irradiation may affect tumor response.

Authors' Affiliations: [1]Division of Clinical Pharmacology, Departments of Pharmacology and Toxicology, [2]Surgery, [3]Pathology, and [4]Radiation Oncology; and [5]Comprehensive Cancer Center, University of Alabama at Birmingham, Birmingham, Alabama

Received 3/21/05; revised 9/29/05; accepted 10/6/05.

Grant support: NIH grant-1 P20 CA101955-01.

The costs of publication of this article were defrayed in part by the payment of page charges. This article must therefore be hereby marked *advertisement* in accordance with 18 U.S.C. Section 1734 solely to indicate this fact.

Requests for reprints: Martin R. Johnson, Department of Clinical Pharmacology, Wallace Tumor Institute, University of Alabama at Birmingham, Room 620, 1824 6th Avenue South, Birmingham, AL 35294-3300. Phone: 205-975-8435; Fax: 205-975-5650; E-mail: martin.johnson@ccc.uab.edu.

doi:10.1158/1078-0432.CCR-05-0627

Pancreatic cancer, the fourth leading cause of cancer mortality in the United States (1, 2), is characterized by an unusual resistance to both radiation [X-ray therapy (XRT)] and chemotherapy. Despite highly aggressive therapeutic approaches, the overall median survival of 3 to 5 months and a 5-year survival rate of 0.4% to 3% have not appreciably changed in the last 80 years (3). Surgery remains the most effective treatment for pancreatic adenocarcinoma, the most common and malignant type of pancreatic cancer. However, only 10% to 15% of patients have tumors suitable for resection, and 30% to 70% of these patients will have local recurrences (4, 5). At the time of diagnosis, most patients have locally advanced or metastatic disease with involvement of the peritoneum, liver, lungs, or

DOI:10.1158/1078-0432.CCR-05-0627

lymph nodes. Chemoradiotherapy with either 5-fluorouracil (5-FU; ref. 6) or, more recently, gemcitabine (7, 8), has become the most commonly used treatment modality. The current approach using XRT is to reduce the amount of toxicity to adjacent tissues by focusing treatment to the primary tumor area, the area of residual tumor, or the site of tumor excision (involved fields or intensity-modulated radiation therapy). However, the effect of localized XRT on metastatic tumors outside the irradiated field (abscopal effects), particularly in combination with chemotherapy, remains to be elucidated.

The term "abscopal" was first introduced by Mole (9) in 1953 to describe the effects of localized XRT on distant tissue that is outside the field of radiation absorption. It should be clarified that this phenomenon does not refer to bystander effects, mediated by gap-junction intracellular communication (10), but refers to radiation responses seen in areas separate from the irradiated tissue, mediated by the secretion of soluble factors from irradiated cells. Elucidation of the precise molecular components and mechanisms responsible for such abscopal effects remains an active area of investigation that is further complicated by conflicting reports of either proliferative or antitumor effects in cells outside the field of irradiation (11–16). Whereas antiproliferative abscopal effects have been attributed to circulating lymphocytes, cytokines, or immune mediators, proliferative effects have been suggested to occur via activation of matrix metalloproteinases and growth factors (11, 12, 14–17). In addition, although abscopal effects have been reported in a variety of malignancies, including lymphoma, papillary adenocarcinoma, melanoma, adenocarcinoma of the esophagus, chronic lymphocytic leukemia, and hepatocellular carcinoma, there have been surprisingly few studies in advanced pancreatic adenocarcinoma, where chemoradiotherapy is often used and progression of metastatic disease is widespread.

Previous studies by our laboratory examining the correlation between drug-metabolizing enzymes and potential efficacy to fluoropyrimidine chemotherapy in combination with radiation therapy showed abscopal effects in contralateral lead-shielded xenografts (18). These studies, combined with tumor tissue analysis suggesting response to capecitabine based on the expression of the indicators of response thymidine phosphorylase and dihydropyrimidine dehydrogenase, provided the rationale for two phase I clinical trials at our institution examining concurrent administration of capecitabine and XRT for the treatment of both glioblastoma multiforme and pancreatic adenocarcinoma (19, 20).

In the current study, we examine the effect of XRT alone and in combination with capecitabine and/or celecoxib in both irradiated and lead-shielded contralateral BxPC-3 xenografts. This model, consisting of animals containing both an irradiated and a distant tumor outside the field of irradiation, was used to represent metastatic disease. The addition of celecoxib was chosen based on our preliminary molecular analysis of surgically resected pancreatic adenocarcinoma biopsies demonstrating cyclooxygenase-2 (COX-2) overexpression, a marker of tumor progression and invasion. Taken collectively with previous studies demonstrating the abscopal effects of XRT, the radiosensitizing properties of 5-FU in pancreatic cancer (21), a selective increase of thymidine phosphorylase levels following XRT (18, 22), and the potential benefits of COX-2 inhibition (23), our examination of this trimodal regimen may be potentially useful in establishing future treatment paradigms for pancreatic cancer.

Materials and Methods

Tissue preparation. Following an Institutional Review Board–approved protocol, primary pancreatic ductal adenocarcinoma ($n = 5$) and uninvolved (normal) pancreatic tissues ($n = 5$) were obtained from cancer patients undergoing surgical resection. Tissues to be used for RNA extraction were snap frozen in liquid nitrogen and stored at −80°C. Before RNA extraction, a 5 μm section was obtained from frozen tissue that had been fixed and paraffin embedded; it was then stained with H&E so that it could be examined by a pathologist to confirm a diagnosis.

RNA extraction. Total RNA was isolated using the Qiagen RNA Purification kit following instructions of the manufacturer (Qiagen, Valencia, CA). All sample concentrations were determined spectrophotometrically at A_{260} and diluted to a final concentration of 20 ng/μL in RNase-free water containing 12.5 ng/μL of total yeast RNA (Ambion, Austin, TX) as a carrier.

Real-time quantitative PCR. Expression levels were determined using an ABI 7900 Sequence Detection System as previously described by our laboratory (24, 25). The real-time quantitative PCR primers were as follows: human thymidine phosphorylase forward (5′-TCCTGCGGACGGAATCC-3′), reverse (5′-TGAGAATGGAGGCTGTGATGAG-3′), and fluorophore-labeled probe (FAM-CAGCCAGAGATGTGACAGCCACCGT-TAMRA); COX-2 forward (5′-GAATCATTCACCAGGCAAATTG-3′), reverse (5′-TCTGTACTGCGGGTGGAACA-3′), and probe (FAM-TGGCAGGGTTGCTGGTGGTAGGA-TAMRA). The sequence for the primers and probes for human dihydropyrimidine dehydrogenase and S9 ribosomal have been previously described (18, 25). Expression levels were calculated using the relative standard curve method (24, 25). All reactions were run in triplicate and standard curves with correlation coefficients falling below 0.98 were repeated. Control reactions confirmed that no amplification occurred when yeast total RNA was used as a template or when no-template-control reactions were done.

Immunohistochemistry. Thymidine phosphorylase protein levels were evaluated in pancreatic adenocarcinoma, uninvolved pancreas, colorectal carcinoma, and normal mucosa by immunohistochemistry using the Antithymidine Phosphorylase Antibody, Formalin-Grade kits according to the instructions of the manufacturer (Roche Diagnostics, Mannheim, Germany). Briefly, 5 μm sections were deparaffinized and rehydrated before undergoing antigen retrieval by steaming for 5 minutes. Sections were blocked with 20% normal goat serum for 20 minutes before overnight incubation at 4°C with thymidine phosphorylase antibody/antiserum at a dilution of 1:100. Secondary Envision+ peroxidase antibody (DAKO, Inc., Glostrup, Denmark), specifically antimouse for thymidine phosphorylase, was added to the sections for 30 minutes before color development with liquid diaminobenzidine tetrachloride (DAKO) for 20 minutes and counterstaining with Mayer's hematoxylin. Between each incubation step, sections were washed twice with 1× PBS for 5 minutes. A negative control section without the addition of thymidine phosphorylase–specific antibody was included for each case. Immunostains were assessed based on their intensity.

Ki-67 immunohistochemistry in BxPC-3 xenografts on day 50. We determined the proliferation index of both irradiated and shielded xenograft samples immunohistochemially, by analyzing the expression of Ki-67 as previously described (26–28). Briefly, 5-μm-thick tissue sections were obtained from formalin-fixed, paraffin-embedded tissue and placed on SuperFrost/Plus slides (Fisher Scientific, Norcross, GA), deparaffinized in xylene, and subsequently rehydrated in graded ethanol. Antigen retrieval was then done by steaming for 5 minutes in a 0.01 mol/L EDTA (pH 8) solution. The sections were then transferred to a Tris-buffer bath [0.05 mol/LTris base, 0.15 mol/L

DOI:10.1158/1078-0432.CCR-05-0627

NaCl, and 0.01% Triton X-100 (pH 7.6)]. Each section was treated with an aqueous solution of 3% H_2O_2 for 5 minutes to quench endogenous peroxidase activity. Sections were then incubated with 3% goat serum at room temperature for 20 minutes to reduce nonspecific immunostaining. The primary antibody used was an anti Ki-67 rabbit monoclonal antibody (clone: SP6, LabVision Co., Fremont, CA, dilution: 1:400). Negative controls were done by omitting the primary antibodies. Sections from tonsils served as positive controls. Secondary detection was accomplished using the USA-Ultra Streptavidin Detection System (Signet, Inc., Dedham, MA). The sections were exposed to a biotinylated antirabbit antibody for 20 minutes and a peroxidase-conjugated streptavidin was added for 20 minutes. A diaminobenzidine tetrachloride (BioGenex, San Ramon, CA) chromogen was used to visualize the antibody-antigen complex. Each section was then counterstained using hematoxylin, dehydrated using graded alcohols, and soaked in xylene before coverslipping. The slides were examined by a pathologist (D.C. Chhieng). Positive staining was defined as the presence of nuclear staining regardless of intensity. The proportion of tumor cells that showed nuclear staining was estimated as a percentage of total tumor cells.

Cell culture. BxPC-3 pancreatic carcinoma cells (purchased from the American Type Culture Collection, Manassas, VA) were maintained in stationary monolayer cultures at 37°C and 5% CO_2 in a humidified atmosphere using RPMI supplemented with 10% heat-inactivated fetal bovine serum and 2.6 mmol/L L-glutamine. The BxPC-3 cell line was used due to its high expression of COX-2 (29). All cell cultures were maintained in antibiotic-free conditions and regularly checked for *Mycoplasma* contamination using a PCR-based kit (American Type Culture Collection). Near-confluent (75%) monolayers of cells were harvested by brief exposure to 0.05% trypsin/0.53 mmol/L EDTA (Life Technologies, Gaithersburg, MD). Harvested cells were pelleted (200 × *g*, 8 minutes at ambient temperature) in complete medium and resuspended in serum-free medium. Viable cells were counted using a Neubauer hemacytometer and trypan blue (0.4%) exclusion.

Pancreatic cancer xenograft preparation and irradiation. Athymic, nude NCr mice (*nu/nu*) were subcutaneously injected, bilaterally into hind flanks with a suspension of 1×10^7 BxPC-3 pancreatic cancer cells (Fig. 1). Tumors were allowed to develop between 35 and 40 mm^2 in size (28 days postinjection). Tumor surface area was determined with vernier calipers by multiplying the length of the tumors by their width and tumor growth was monitored twice per week. Mice were randomized into control and treatment groups with each group containing 12 to 15 mice. One of the pancreatic tumor-bearing flanks of the treated group was irradiated, whereas the rest of the mouse (including the liver and the tumor in the contralateral flank) was lead shielded (illustrated in Fig. 1). XRT was carried out using a ^{60}Co teletherapy X-ray unit (Picker, Cleveland, OH) and was administered (2 Gy for 5 consecutive days) on day 0 (start of treatment day, which occurred 28 days after cell injection) and day 24. Mice in control groups were anesthetized with ketamine/zyloxine but were not irradiated. Capecitabine (Xeloda, Hoffmann-La Roche, Inc., Nutley, NJ) was dissolved in 40 mmol/L citrate buffer (pH 6.0)/5% gum Arabic and administered by gavage at a dose of 350 mg/kg for 14 consecutive days (days 0-13), followed by 10 days of rest before administration of the second, 14-day treatment cycle (days 24-37). Celecoxib (Celebrex, Pfizer, New York, NY) was incorporated in the diet at 100 ppm (equivalent to 20 mg/kg/d p.o.); feed was weighed daily and continuously administered throughout the duration of the 50-day study. Mice were sacrificed at various time points (0, 4, 12, 24, 32, 45, and 50 days) throughout the study for tissue analysis (gene expression and immunohistochemistry).

Statistical analysis. To evaluate differences in gene expression between normal and tumor tissues, paired *t* tests were done where α was set at 0.05. The tumor growth curve data were analyzed by a log-linear mixed model approach on repeated measures ANOVA, using the MIXED procedure in SASR (30, 31). To determine if any combination therapy arms produced significant synergistic inhibition of tumor growth (i.e., more than additive), the tumor growth curves from the serial area (log) measurements were compared using a two-way repeated measures analysis. To test for synergistic effects of the combination therapies, an interaction term was included in the model. If the interaction term was significant and the effect was inhibition of growth at a rate greater than additive, then the interaction was considered synergistic. The mean tumor tripling times were analyzed using the Kruskal-Wallis test and Fisher's exact test was used to compare the proportions of tumor size decrease.

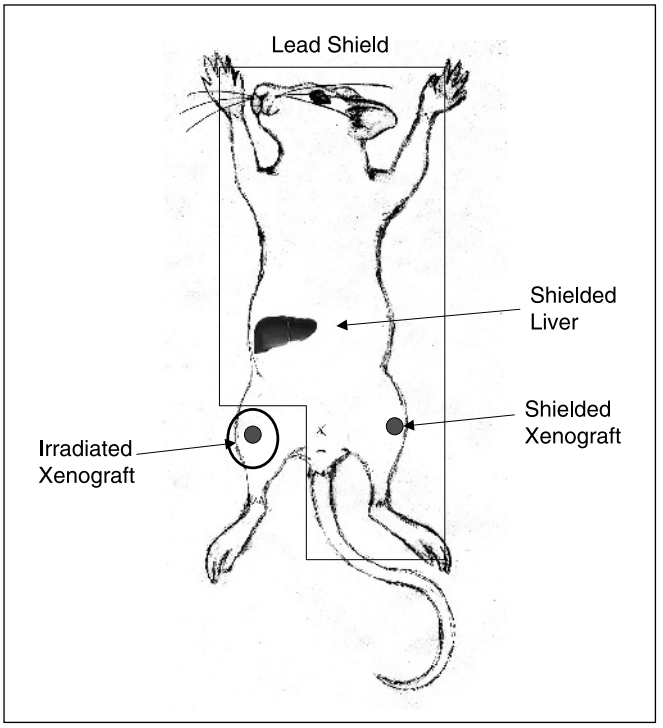

Fig. 1. Schematic of mouse xenograft location(s) and irradiation. One of the two flanks containing a BxPC-3 xenograft was irradiated (*circled*), whereas the contralateral flank (containing the other BxPC-3 xenograft) as well as the body of the mouse was lead shielded.

Results

Quantitation of thymidine phosphorylase, dihydropyrimidine dehydrogenase, and cyclooxygenase-2 expression in pancreatic adenocarcinoma and normal pancreatic tissues. As shown in Fig. 2, thymidine phosphorylase expression is ~7.5-fold higher in pancreatic adenocarcinoma (mean = 41.7; SE = 8) compared with normal pancreatic tissue (mean = 5.5; SE = 1.5) with a mean difference of 36.2. These differences were statistically significant ($P < 0.05$). There was no statistically significant difference in dihydropyrimidine dehydrogenase levels between normal (mean = 12.5; SE = 5) and tumor tissue samples (mean = 10; SE = 3.5) with a mean difference of 2.6 ($P > 0.05$). The average thymidine phosphorylase/dihydropyrimidine dehydrogenase ratio shown in pancreatic adenocarcinoma (4.2) is ~9.4-fold higher than that of normal pancreatic tissue (0.4). The higher ratio in pancreatic adenocarcinoma was primarily due to higher expression of thymidine phosphorylase compared with normal pancreas ($P < 0.05$). COX-2 mRNA levels in pancreatic adenocarcinoma (mean = 22.2; SE = 11.9) were >100-fold higher compared with normal pancreas (mean = 0.2;

DOI:10.1158/1078-0432.CCR-05-0627

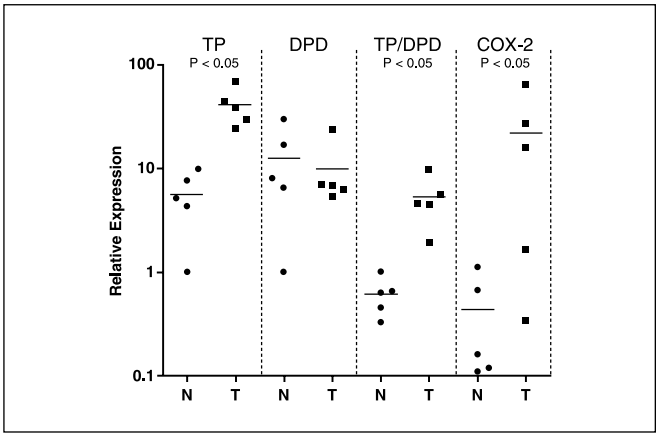

Fig. 2. Expression of thymidine phosphorylase (*TP*), dihydropyrimidine dehydrogenase (*DPD*), and COX-2 mRNA in uninvolved pancreatic tissue (*N*) and pancreatic adenocarcinoma (*T*). Thymidine phosphorylase expression is 7.5-fold higher in pancreatic adenocarcinoma (■) compared with normal pancreas (●). There was no significant difference in dihydropyrimidine dehydrogenase expression levels in the same tissue samples. The average thymidine phosphorylase/dihydropyrimidine dehydrogenase ratio shown in pancreatic adenocarcinoma is ~9.4-fold higher than that of normal pancreas and is primarily due to thymidine phosphorylase overexpression. This profile should result in selective conversion of capecitabine (into 5-FU) in tumor compared with normal pancreatic tissues. COX-2 expression is over 100-fold higher in pancreatic adenocarcinoma compared with normal pancreatic tissue.

SE = 0.1), with a mean difference of 22 ($P < 0.05$). Greater range in COX-2 expression in tumor tissue relative to normal tissue was also observed.

Immunohistochemistry of pancreatic adenocarcinoma, uninvolved pancreas, colorectal carcinoma, and normal mucosa. To determine whether the increased thymidine phosphorylase mRNA levels in pancreatic adenocarcinoma correlated with protein levels, immunohistochemistry was done on pancreatic adenocarcinoma and uninvolved pancreas. Because capecitabine is approved for colorectal carcinoma and previous studies have suggested that thymidine phosphorylase up-regulation in several gastrointestinal malignancies (including colorectal carcinoma) is mainly attributed to the stromal compartment, immunohistochemistry was also done in colorectal carcinoma and normal mucosa as a reference for comparison to pancreatic adenocarcinoma. As shown in Fig. 3, thymidine phosphorylase staining in uninvolved pancreatic tissue (Fig. 3A) showed few areas of faint staining, predominantly in the cytoplasm of the acinic cells and focally in the cytoplasm of the ductal cells. Scattered staining of thymidine phosphorylase can also be observed in the surrounding stroma. In Fig. 3B (pancreatic adenocarcinoma), however, strong thymidine phosphorylase–specific immunoreactivity is observed in the neoplastic ducts of a well-differentiated pancreatic ductal carcinoma. Although stromal cells also showed faint and scattered staining of thymidine phosphorylase, in pancreatic adenocarcinoma (Fig. 3B), intense and diffuse cytoplasmic staining is observed in the ductal adenocarcinoma cells. Figure 3C (*bottom left*) shows thymidine phosphorylase staining in normal mucosa relative to colorectal carcinoma (D). In the normal mucosa (C), thymidine phosphorylase expression is noted predominantly in the stroma. In contrast to pancreatic tissue, no staining is noted in the colonic crypts here. Figure 3D shows thymidine phosphorylase staining in colorectal carcinoma. Several gastrointestinal malignancies, such as colorectal carcinoma (D), and unlike pancreatic adenocarcinoma (B), show thymidine phosphorylase expression that is predominantly localized to the stroma (as confirmed here). In addition, colorectal carcinoma shows very weak cytoplasmic staining in the neoplastic glands (thymidine phosphorylase stain, ×100 for all samples).

BxPC-3 tumor xenografts. As illustrated in Fig. 1, athymic NCr mice were s.c. injected with BxPC-3 pancreatic cancer cells in both hind flanks and allowed to develop tumors. To represent metastatic disease, one of the tumor-bearing flanks of the treated groups was irradiated, whereas the rest of the mouse (including the contralateral tumor) was lead shielded.

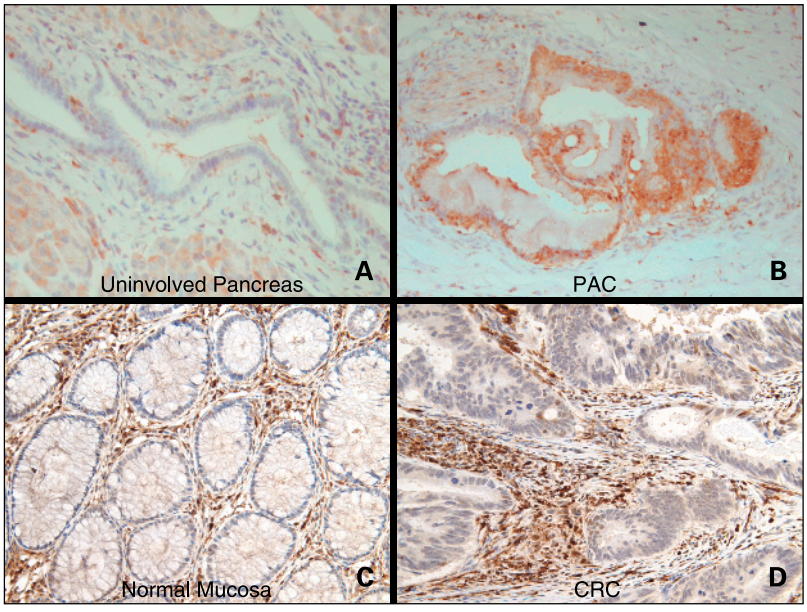

Fig. 3. Immunohistochemical localization of thymidine phosphorylase in pancreatic adenocarcinoma, colorectal carcinoma, and corresponding uninvolved tissues. *A,* uninvolved pancreatic tissue. Thymidine phosphorylase expression is noted predominantly in the cytoplasm of the acinic and ductal cells as well as scattered staining in the surrounding stroma. *B,* pancreatic ductal carcinoma (*PAC*). Diffuse and intense cytoplasmic thymidine phosphorylase staining is observed in the neoplastic ducts. Scattered staining of thymidine phosphorylase is also noted in the surrounding stroma. *C,* thymidine phosphorylase staining in normal colonic mucosa. Thymidine phosphorylase expression is noted predominantly in the stroma. In contrast to pancreatic tissue, no staining is noted in the colonic crypts. *D,* colonic carcinoma (*CRC*) tissue. Intense thymidine phosphorylase expression is noted in the surrounding stroma with very weak cytoplasmic staining in the neoplastic glands (thymidine phosphorylase stain magnification, ×100 for all samples).

DOI:10.1158/1078-0432.CCR-05-0627

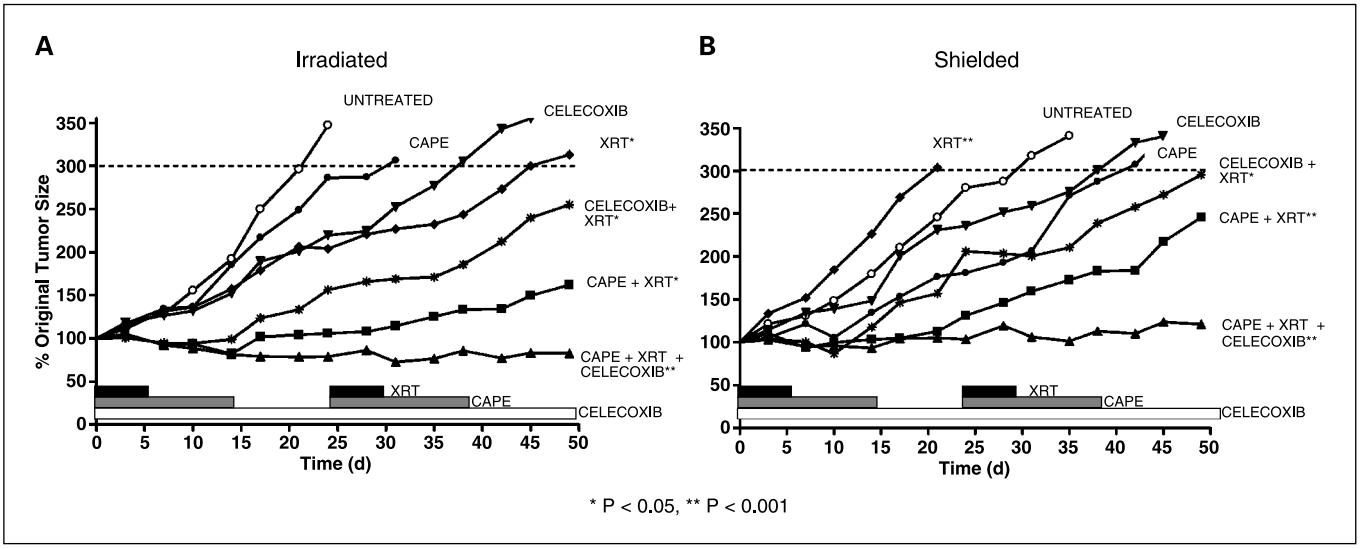

Fig. 4. Percentage change in tumor surface area versus time in both irradiated (*A*) and shielded contralateral (*B*) BxPC-3 xenografts. Treatment schedule throughout the duration of study [—, XRT; ═, capecitabine (CAPE); ═, celecoxib]. *, $P < 0.05$; ** $P < 0.001$. *A,* monotherapy with capecitabine, celecoxib, or XRT. Only treatment with XRT produced a significant reduction in tumor area ($P < 0.05$). The combination of capecitabine and fractionated XRT showed antiproliferative synergy ($P = 0.008$). The trimodal combination (capecitabine-XRT-celecoxib) was the most effective regimen, maximally decreasing tumor area by 27% ($P < 0.001$). *B,* proliferative abscopal effects of XRT promoted growth by 23% in contralateral lead-shielded tumors within the same animals. Monotherapy with capecitabine or celecoxib was not significantly different from untreated tumors ($P > 0.05$). The celecoxib and contralateral XRT combination did not produce a significant antiproliferative effect ($P > 0.05$). However, shielded xenografts showed antitumor synergy with capecitabine and contralateral XRT ($P < 0.001$). Similar to irradiated xenografts, the trimodal combination was also the most effective regimen despite these tumors being outside the field of irradiation ($P < 0.001$).

Figure 4 shows the results of treatment with capecitabine, XRT, and/or celecoxib alone and in combination on tumor surface area in both irradiated (A) and lead shielded, contralateral xenografts (B).

Irradiated tumors. As shown in Fig. 4A, untreated tumors showed tripling times of ~20 days. In these xenografts, monotherapy suggested that XRT was the most effective treatment, followed by celecoxib, and capecitabine with tripling times of 44, 36, and 28 days, respectively. However, only XRT achieved statistically significant differences from untreated controls ($P < 0.05$) with 33% of the mice responding to treatment. The combination of celecoxib and XRT produced an additive and statistically significant inhibition of tumor growth ($P < 0.05$; 33% response). However, the combination of capecitabine and XRT produced a synergistic inhibition of tumor growth ($P = 0.008$; 75% response), which was further improved with the addition of celecoxib ($P < 0.001$; 92% of mice responding). As shown in Fig. 4A, combination (both dual and trimodal) therapy prevented tumors from tripling and, therefore, tumor surface area was used to determine response. The celecoxib-XRT and the capecitabine-XRT combinations produced maximal reductions in tumor area (set at 100% at the start of treatment) to 94% and 82%, respectively. However, the trimodal combination of XRT-capecitabine-celecoxib was the most effective regimen (Fig. 4A), maximally decreasing tumor area to 73% of the original size ($P < 0.001$).

Contralateral, lead-shielded tumors (abscopal effects). In this model, lead-shielded tumors were also evaluated to determine whether abscopal effects of XRT occurred. As shown in Fig. 4B, untreated contralateral tumors showed tripling times of ~27 days. The differences in tripling times between untreated tumors (20 days on one side versus 27 days on the contralateral side) were not statistically significant ($P > 0.05$). Monotherapy with either celecoxib or capecitabine did not show significant differences from untreated tumors ($P > 0.05$). Independently, capecitabine and celecoxib showed tripling times of 41 and 36 days, respectively (17% and 14% of the mice responding to treatment, respectively), compared with 27 days for untreated tumors ($P > 0.05$). However, whereas monotherapy with XRT showed significant antitumor effects in irradiated xenografts, in lead-shielded contralateral tumors, proliferative abscopal effects were observed. Specifically, contralateral XRT significantly promoted growth by 23% (compared with untreated tumors) in these shielded tumors outside the irradiated field ($P < 0.001$). Surprisingly, when capecitabine was included with distant, contralateral XRT (which was not directly administered to these tumors but rather, to the contralateral flanks only), these lead-shielded tumors also showed a significant synergistic inhibition of growth as evaluated by early growth curve analysis ($P < 0.001$; 58% response). As with irradiated xenografts, the addition of celecoxib further inhibited tumor growth ($P < 0.001$), making this the most effective regimen evaluated with 83% of the mice responding to this treatment regimen. Direct comparison using statistical analysis between the trimodal combination therapy and the bimodal combinations revealed that the triple therapy had significantly reduced tumor growth ($P < 0.001$). Further, the tumor growth inhibition was sustained, preventing tumor growth up to day 50 despite these tumors not having received direct irradiation. However, no eradication of tumor was observed for any of the mice (including those receiving the trimodal combination, whether they were shielded or directly irradiated).

In a separate experiment, concurrent treatment with capecitabine and celecoxib (no XRT) showed additive antiproliferative efficacy and suggest the synergy observed in both irradiated and contralateral shielded xenografts with concurrent administration of capecitabine + celecoxib cannot be attributed to the capecitabine-celecoxib combination.

DOI:10.1158/1078-0432.CCR-05-0627

Proliferation index of BxPC-3 xenografts as measured by Ki-67 expression. The effect of treatment on proliferation was evaluated by determining Ki-67 expression in xenografts harvested on day 50 using immunohistochemistry. The proliferation index is expressed as a percentage of positive nuclear staining (with Ki-67) in tumor cells. As shown in Fig. 5A and D, untreated xenografts showed ~50% and 40% positive staining for Ki-67. In irradiated xenografts (Fig. 5B), there was no significant change in Ki-67 compared with untreated groups (Fig. 5A and D) with ~35% of the tumor cells staining positive. However, in lead-shielded xenografts in the same animals, where an abscopal proliferative effect was observed *in vivo* (see Fig. 4B), ~70% of the tumor cells expressed Ki-67 (Fig. 5E). For both irradiated (Fig. 5C) and lead-shielded xenografts (Fig. 5F), trimodal combination (capecitabine-XRT, or capecitabine-contralateral XRT and celecoxib) caused an appreciable reduction in Ki-67 expression with only 10% and 17% of the tumor cells demonstrating positive Ki-67 staining.

Quantitation of thymidine phosphorylase, dihydropyrimidine dehydrogenase, and cyclooxygenase-2 mRNA in BxPC-3 xenografts. Thymidine phosphorylase and dihydropyrimidine dehydrogenase mRNA levels did not change significantly in any of the treatment groups, including XRT ($P > 0.05$), for either irradiated or lead-shielded tumors (data not shown). COX-2 mRNA was also not significantly affected by XRT or capecitabine ($P > 0.05$); however, celecoxib administration to dual combination therapy showed a trend in decreased COX-2 expression of 2-fold, which was not statistically significant (data not shown; $P > 0.05$).

Discussion

Pancreatic cancer remains one of the most lethal gastrointestinal tumors with an average survival of only 4 to 6 months and an overall 5-year survival of <10% (1, 3). Despite improved endoscopic diagnostic methods (32) and aggressive treatment regimens, only small incremental improvements in overall survival have been achieved (3). This failure to develop an effective treatment for pancreatic adenocarcinoma combined with recent advances in our ability to perform molecular analysis in biopsy-sized tissue samples has provided the impetus to design novel treatment regimens based on the molecular profile of the tumor.

Previous studies in human colon and breast cancer xenograft models have suggested that expression of thymidine phosphorylase and dihydropyrimidine dehydrogenase can be used to assess response to capecitabine (a recently introduced orally administered fluoropyrimidine prodrug that mimics continuous infusional 5-FU; ref. 33). Increased thymidine phosphorylase (the final and rate-limiting metabolic step in the conversion of capecitabine into 5-FU) has been shown to result in higher intratumoral levels of 5-FU (34, 35). Preclinical studies have also shown synergistic antitumor efficacy with concomitant administration of capecitabine and XRT (22). The molecular basis for synergy has been attributed to an induction of thymidine phosphorylase following XRT. Previous studies by our laboratory showed increased thymidine phosphorylase expression in both irradiated and distant, contralateral lead-shielded xenografts (18). Collectively, these data offer the exciting possibility that metastatic or micrometastatic tumors outside the field of irradiation could become more sensitive to capecitabine (via abscopal effects). In the current study, the antitumor efficacy of XRT alone and in combination with capecitabine and/or celecoxib was examined in both irradiated and lead-shielded, contralateral BxPC-3 pancreatic cancer xenografts.

Initial studies examining pancreatic adenocarcinoma biopsies showed statistically significant overexpression of thymidine phosphorylase and COX-2 in tumor compared with uninvolved pancreas (Fig. 2; ref. 36). There were no

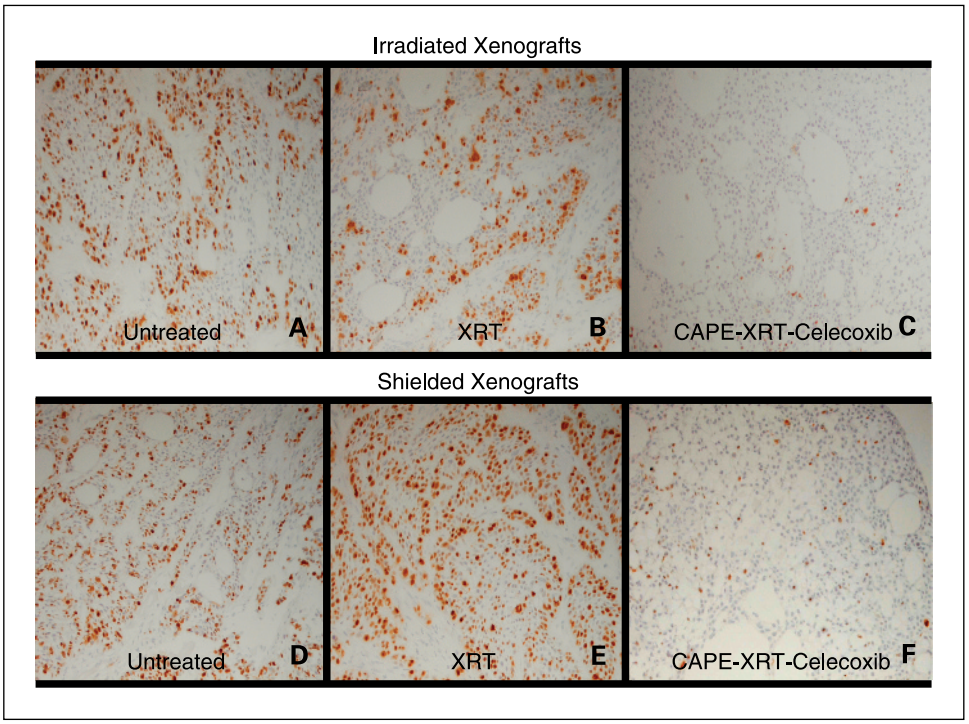

Fig. 5. Immunohistochemistry of Ki-67 expression at day 50 is shown in irradiated (*top*) and shielded (*bottom*) BxPC-3 xenografts. As shown, untreated tumors (*A* and *D*) showed Ki-67 staining in ~50% and 40% of the tumor cells, respectively. In irradiated tumors (*B*), 35% of the cells expressed Ki-67 similar to untreated controls. In tumors receiving the trimodal combination (capecitabine, XRT, and celecoxib), proliferation was dramatically reduced (*C*) where only 10% of the cells stained positive for Ki-67. In shielded, contralateral tumors, 70% of the cells stained positive for Ki-67 proliferation marker (*E*). In shielded tumors receiving contralateral XRT-capecitabine and celecoxib, only 17% of the cells showed Ki-67 expression (*F*), despite these tumors being outside the irradiation field (×100 magnification for all samples).

DOI:10.1158/1078-0432.CCR-05-0627

significant differences in dihydropyrimidine dehydrogenase expression (Fig. 2). Concordance between elevated thymidine phosphorylase mRNA and protein levels was confirmed by immunohistochemistry, which showed that thymidine phosphorylase protein was localized to the ductal tumor cells in pancreatic adenocarcinoma (Fig. 3). This is in contrast to colorectal carcinoma (a cancer type for which capecitabine is approved for), where thymidine phosphorylase is mainly localized to the stroma (Fig. 3D). Based on previous pharmacokinetic studies, this distribution of thymidine phosphorylase and dihydropyrimidine dehydrogenase in pancreatic adenocarcinoma should result in selective intratumoral activation of capecitabine into 5-FU (elevated thymidine phosphorylase), whereas 5-FU clearance from tumor and normal tissues should be similar (equivalent dihydropyrimidine dehydrogenase levels; refs. 22, 34, 37). Further, localization of thymidine phosphorylase to the pancreatic adenocarcinoma tumor cells suggests that capecitabine would be more suitable for pancreatic adenocarcinoma than colorectal carcinoma in targeting the tumor cells. Collectively, these data provided the rationale for examining a multimodality treatment regimen in a preclinical animal model using capecitabine, XRT, and celecoxib. Results obtained from this study were used in the design of an ongoing phase I clinical trial examining concurrent administration of capecitabine with XRT in locally advanced pancreatic adenocarcinoma patients (20).

The xenograft model used in this study (with each animal containing contralateral tumors), although limited in that it is not truly a metastatic model, was designed to represent metastatic, and/or micrometastatic disease in humans where the "primary" tumor is irradiated and the "secondary" tumor remains outside the field of XRT (Fig. 1; ref. 18).

To better represent metastasis, orthotopic xenograft mouse models (using cell lines that metastasize from the primary site of injection) could be used as valuable tools for improving our understanding of metastatic disease. Nevertheless, our model provided useful information on the effects of XRT on distant tumors shielded from direct XRT. In irradiated xenografts, monotherapy suggested XRT was the most effective treatment, followed by celecoxib and capecitabine. However, only XRT achieved statistically significant differences from untreated controls (Fig. 4). The combination of capecitabine and XRT showed synergistic antiproliferative efficacy that was further improved with the addition of celecoxib (Fig. 4). This trimodal combination showed the greatest antiproliferative efficacy by preventing tumor growth throughout the duration of the study (stabilizing the disease), and, in fact, maximally decreasing tumor size by 27% (Fig. 4A). The single, dual, and trimodal therapy combinations used in this study showed low toxicity with no animal deaths or significant changes in body weight (>10% from baseline) throughout the duration of the experiment. However, none of these combinations was able to completely eradicate the tumors. Interestingly, in subsequent studies using tunnel immunohistochemistry to determine apoptosis, although slightly greater apoptosis was observed with the addition of celecoxib, this effect was not significantly different from untreated tumors. Ideally, prostaglandin E_2 levels should have been evaluated to determine the effects of celecoxib inhibition of COX-2 activity in every mouse receiving celecoxib therapy (38).

Interestingly, abscopal effects were observed in lead-shielded contralateral tumors in the same animals. Monotherapy with XRT showed proliferative effects (increasing tumor size by 23%) in lead-shielded tumors outside the field of irradiation (Fig. 4B). Although XRT is not typically administered as monotherapy, these results may explain the basis for a previous clinical study, which suggested that the median survival time for pancreatic adenocarcinoma patients with distant metastasis who were treated with intraoperative radiotherapy is shorter than that of the control group (39). Of particular interest, when capecitabine is introduced, contralateral XRT shows synergistic, antiproliferative efficacy, despite these xenografts being outside the irradiated field. Furthermore, the combination of capecitabine-contralateral XRT was nearly (but not quite) as effective as the capecitabine-XRT combination evaluated in irradiated xenografts (Fig. 4A) and was also improved with the addition of celecoxib (Fig. 4B). It is noteworthy that although capecitabine-XRT was better than celecoxib-XRT in irradiated tumors, in shielded tumors, capecitabine-XRT had nearly the same antiproliferative effect as celecoxib-XRT. It is known that XRT induces certain inflammatory cytokines, which, in turn, can up-regulate COX-2 expression (40). Previous reports have shown that COX-2 is inducible, particularly during inflammatory states involving cytokines (41, 42). However, these differences were not statistically significant, and, further, we did not see COX-2 mRNA up-regulation in these xenografts. COX-2 protein levels would need to be examined to determine whether increased COX-2 protein may be a reason for the differences of celecoxib-XRT between irradiated and shielded tumors.

Immunohistochemical analyses of Ki-67 expression showed concordance with tumor area results, where, as a result of abscopal XRT, significantly higher expression was observed in contralateral shielded tumors compared with untreated BxPC-3 xenografts (Fig. 5). Irradiated and contralateral shielded tumors receiving the trimodal combination showed the lowest Ki-67 expression (Fig. 5). These results may have significant clinical implications in the rational design of treatment regimens for pancreatic cancer where XRT is used in patients with metastatic tumors outside the field of irradiation.

Surprisingly, the synergism observed with capecitabine and concomitant XRT could not be attributed to elevated thymidine phosphorylase levels in either irradiated or contralateral shielded xenografts. A recent study examining thymidine phosphorylase levels before and after XRT in endoscopic biopsies obtained from patients with locally advanced pancreatic adenocarcinoma also showed no significant induction of thymidine phosphorylase secondary to XRT (20). Similar results were recently reported in cervical squamous cell carcinoma (43). Collectively, these data suggest that the increased thymidine phosphorylase expression observed following XRT in some tumor types (breast, colorectal, and glioma; ref. 22) may be cell specific. Further, additional genes that have been associated with response to fluoropyrimidine therapy (including orotate phosphoribosyl transferase and thymidylate synthase) may need to be examined to clarify the synergistic antiproliferative efficacy of capecitabine and XRT (44–48). Recent advances in the ability to quantify gene expression levels (real-time, low-density array analysis) will allow the simultaneous examination of all known anabolic and catabolic enzymes involved in the metabolism of

DOI:10.1158/1078-0432.CCR-05-0627

fluoropyrimidines and may clarify the molecular basis for response (49).

Elucidating the molecular basis responsible for abscopal effects has been complicated by conflicting reports in the literature, suggesting that abscopal XRT can have either proliferative or antiproliferative effects in tumor cells outside the field of irradiation. Proliferative effects have been attributed to an induction of matrix metalloproteinases, growth factors, or up-regulation of the c-Met pathway in pancreatic cancer cells, which promote the malignant and proliferative phenotype of pancreatic cancer (14, 17). Antiproliferative effects have been suggested to occur by local irradiation causing a cytokine-mediated antitumor effect (13). Unfortunately, the small number of clinical reports describing abscopal effects in patients remains primarily descriptive (12, 13, 50). In the current study, XRT showed proliferative effects on distant xenografts outside the field of irradiation and may be the basis for the observed increase in sensitivity following administration of capecitabine because antineoplastics have been shown to be more effective in actively dividing cells.

The current study suggests a potentially efficacious trimodality regimen for the treatment of pancreatic adenocarcinoma where synergistic antiproliferative efficacy was shown in irradiated xenografts with coadministration of capecitabine. This combination was further improved following the addition of celecoxib. However, molecular analysis suggests that efficacy cannot be predicted solely from previously identified indicators of response, including thymidine phosphorylase and dihydropyrimidine dehydrogenase. Interestingly, in xenografts outside the field of irradiation, abscopal effects were observed where (*a*) increased proliferation was shown in the absence of capecitabine and (*b*) synergistic antitumor efficacy occurred following capecitabine administration (which was also improved with celecoxib). These studies suggest that celecoxib may improve outcome in ongoing clinical trials examining capecitabine with concurrent XRT (20).

Altogether, these results have implications in the rational design of treatment paradigms for pancreatic adenocarcinoma where abscopal effects remain largely unknown and metastatic disease is prevalent.

Acknowledgments

We thank Jessica M. Grunda, Kangshang Wang, Adam Lee, Adam Steg, William E. Grizzle, and Kim Hazelwood for their technical support.

References

1. Landis SH, Murray T, Bolden S, Wingo PA. Cancer statistics, 1999. CA Cancer J Clin 1999;49:8–31.
2. Sohn TA. The molecular genetics of pancreatic ductal carcinoma. Minerva Chir 2002;57:561–74.
3. Brasiuniene B, Juozaityte E, Brasiunas V, Inciura A. [The update on pancreatic cancer chemotherapy]. Medicina (Kaunas) 2003;39:1016–25.
4. Beger HG, Rau B, Gansauge F, Poch B, Link KH. Treatment of pancreatic cancer: challenge of the facts. World J Surg 2003;27:1075–84.
5. Penberthy DR, Rich TA, Adams RB. Postoperative adjuvant therapy for pancreatic cancer. Semin Surg Oncol 2003;21:256–60.
6. Moertel CG, Frytak S, Hahn RG, et al. Therapy of locally unresectable pancreatic carcinoma: a randomized comparison of high dose (6000 rads) radiation alone, moderate dose radiation (4000 rads + 5-fluorouracil), and high dose radiation + 5-fluorouracil: The Gastrointestinal Tumor Study Group. Cancer 1981;48:1705–10.
7. Wolff RA, Evans DB, Gravel DM, et al. Phase I trial of gemcitabine combined with radiation for the treatment of locally advanced pancreatic adenocarcinoma. Clin Cancer Res 2001;7:2246–53.
8. Czito BG, Willett CG, Clark JW, Fernandez Del Castillo C. Current perspectives on locally advanced pancreatic cancer. Oncology (Huntingt) 2000;14:1535–45; discussion 1546, 1549–52.
9. Mole RJ. Whole body irradiation—radiology or medicine? Br J Radiol 1953;26:234–41.
10. Snyder AR. Review of radiation-induced bystander effects. Hum Exp Toxicol 2004;23:87–9.
11. Demaria S, Ng B, Devitt ML, et al. Ionizing radiation inhibition of distant untreated tumors (abscopal effect) is immune mediated. Int J Radiat Oncol Biol Phys 2004;58:862–70.
12. Nobler MP. The abscopal effect in malignant lymphoma and its relationship to lymphocyte circulation. Radiology 1969;93:410–2.
13. Ohba K, Omagari K, Nakamura T, et al. Abscopal regression of hepatocellular carcinoma after radiotherapy for bone metastasis. Gut 1998;43:575–7.
14. Qian LW, Mizumoto K, Inadome N, et al. Radiation stimulates HGF receptor/c-Met expression that leads to amplifying cellular response to HGF stimulation via upregulated receptor tyrosine phosphorylation and MAP kinase activity in pancreatic cancer cells. Int J Cancer 2003;104:542–9.
15. Ohuchida K, Mizumoto K, Murakami M, et al. Radiation to stromal fibroblasts increases invasiveness of pancreatic cancer cells through tumor-stromal interactions. Cancer Res 2004;64:3215–22.
16. Camphausen K, Moses MA, Beecken WD, et al. Radiation therapy to a primary tumor accelerates metastatic growth in mice. Cancer Res 2001;61:2207–11.
17. Qian LW, Mizumoto K, Urashima T, et al. Radiation-induced increase in invasive potential of human pancreatic cancer cells and its blockade by a matrix metalloproteinase inhibitor, CGS27023. Clin Cancer Res 2002;8:1223–7.
18. Blanquicett C, Gillespie GY, Nabors LB, et al. Induction of thymidine phosphorylase in both irradiated and shielded, contralateral human U87MG glioma xenografts: implications for a dual modality treatment using capecitabine and irradiation. Mol Cancer Ther 2002;1:1139–45.
19. Newman AJ, Fiveash J, Rosenfeld S, et al. A phase I study of capecitabine and concurrent radiotherapy (RT) for patients with newly diagnosed glioblastoma multiforme. Proc Am Soc Clin Oncol 2004;23:116.
20. Saif MW, Eloubeidi MA, Russo S, et al. A phase I study of capecitabine with concomitant radiotherapy for patients with locally advanced, unresectable pancreatic cancer: expression analysis of endoscopic ultrasound-guided fine needle aspiration biopsies for genes related to capecitabine response. J Clin Oncol. In press 2005.
21. Fung MC, Takayama S, Ishiguro H, et al. [Chemotherapy for advanced or metastatic pancreatic cancer: analysis of 43 randomized trials in 3 decades (1974–2002)]. Gan To Kagaku Ryoho 2003;30:1101–11.
22. Sawada N, Ishikawa T, Sekiguchi F, Tanaka Y, Ishitsuka H. X-ray irradiation induces thymidine phosphorylase and enhances the efficacy of capecitabine (Xeloda) in human cancer xenografts. Clin Cancer Res 1999;5:2948–53.
23. Crane CH, Mason K, Janjan NA, Milas L. Initial experience combining cyclooxygenase-2 inhibition with chemoradiation for locally advanced pancreatic cancer. Am J Clin Oncol 2003;26:S81–4.
24. Blanquicett C, Johnson MR, Heslin M, Diasio RB. Housekeeping gene variability in normal and carcinomatous colorectal and liver tissues: applications in pharmacogenomic gene expression studies. Anal Biochem 2002;303:209–14.
25. Johnson MR, Wang K, Smith JB, Heslin MJ, Diasio RB. Quantitation of dihydropyrimidine dehydrogenase expression by real-time reverse transcription polymerase chain reaction. Anal Biochem 2000;278:175–84.
26. Manne U, Myers RB, Moron C, et al. Prognostic significance of Bcl-2 expression and p53 nuclear accumulation in colorectal adenocarcinoma. Int J Cancer 1997;74:346–58.
27. Porschen R, Lohe B, Hengels KJ, Borchard F. Assessment of cell proliferation in colorectal carcinomas using the monoclonal antibody Ki-67. Correlation with pathohistologic criteria and influence of irradiation. Cancer 1989;64:2501–5.
28. Grizzle WE, Myers RB, Manne U, Srivastava S. Immunohistochemical evaluation of biomarkers in prostatic and colorectal neoplasia. In: Hanausek M, Walaszek Z, editors. Methods in molecular medicine-tumor marker protocols. Totowa (NJ): Humana Press; 1998. p. 143–60.
29. El-Rayes BF, Ali S, Sarkar FH, Philip PA. Cyclooxygenase-2-dependent and -independent effects of celecoxib in pancreatic cancer cell lines. Mol Cancer Ther 2004;3:1421–6.
30. Littell RC, Milliken GA, Stroup WW, Wolfinger RD. SAS system for mixed models. Cary (North Carolina): SAS Institute, Inc.; 1996.
31. Verbeke G, Molenberghs G, editors. Linear mixed models in practice. A SAS-oriented approach. New York: Springer-Verlag; 1997.
32. Jhala NC, Jhala D, Eltoum I, et al. Endoscopic ultrasound-guided fine-needle aspiration biopsy: a powerful tool to obtain samples from small lesions. Cancer 2004;102:239–46.
33. Pentheroudakis G, Twelves C. The rational development of capecitabine from the laboratory to the clinic. Anticancer Res 2002;22:3589–96.
34. Schuller J, Cassidy J, Dumont E, et al. Preferential activation of capecitabine in tumor following oral administration to colorectal cancer patients. Cancer Chemother Pharmacol 2000;45:291–7.
35. Endo M, Shinbori N, Fukase Y, et al. Induction of thymidine phosphorylase expression and enhancement of efficacy of capecitabine or 5′-deoxy-5-fluorouridine

DOI:10.1158/1078-0432.CCR-05-0627

by cyclophosphamide in mammary tumor models. Int J Cancer 1999;83:127–34.

36. Blanquicett C, Buchsbaum DJ, Vickers SM, et al. Rationale for capecitabine (CAP) and irradiation (XRT) to treat pancreatic cancer. Proc Am Soc Clin Oncol 2003;22:966.

37. Ishikawa T, Sekiguchi F, Fukase Y, Sawada N, Ishitsuka H. Positive correlation between the efficacy of capecitabine and doxifluridine and the ratio of thymidine phosphorylase to dihydropyrimidine dehydrogenase activities in tumors in human cancer xenografts. Cancer Res 1998;58:685–90.

38. Zweifel BS, Davis TW, Ornberg RL, Masferrer JL. Direct evidence for a role of cyclooxygenase 2-derived prostaglandin E_2 in human head and neck xenograft tumors. Cancer Res 2002;62:6706–11.

39. Shibamoto Y, Sasai K, Manabe T. [Radiation therapy of pancreatic cancer]. Gan To Kagaku Ryoho 1992;19:2344–8.

40. Ristimaki A. Cyclooxygenase 2: from inflammation to carcinogenesis. Novartis Found Symp 2004;256:215–21; discussion 221–6, 259–69.

41. Stamp LK, Cleland LG, James MJ. Upregulation of synoviocyte COX-2 through interactions with T lymphocytes: role of interleukin 17 and tumor necrosis factor-α. J Rheumatol 2004;31:1246–54.

42. Wang W, Bergh A, Damber JE. Chronic inflammation in benign prostate hyperplasia is associated with focal upregulation of cyclooxygenase-2, Bcl-2, and cell proliferation in the glandular epithelium. Prostate 2004;61:60–72.

43. Oguri H, Maeda N, Yamamoto Y, Kusume T, Fukaya T. Thymidine phosphorylase expression is preserved after radiotherapy in patients with cervical squamous cell carcinoma. Cancer Chemother Pharmacol 2004;53:151–4.

44. Isshi K, Sakuyama T, Gen T, et al. Predicting 5-FU sensitivity using human colorectal cancer specimens: comparison of tumor dihydropyrimidine dehydrogenase and orotate phosphoribosyl transferase activities with *in vitro* chemosensitivity to 5-FU. Int J Clin Oncol 2002;7:335–42.

45. Leichman CG. Thymidylate synthase as a predictor of response. Oncology (Huntingt) 1998;12:43–7.

46. Metzger R, Danenberg K, Leichman CG, et al. High basal level gene expression of thymidine phosphorylase (platelet-derived endothelial cell growth factor) in colorectal tumors is associated with nonresponse to 5-fluorouracil. Clin Cancer Res 1998;4:2371–6.

47. Salonga D, Danenberg KD, Johnson M, et al. Colorectal tumors responding to 5-fluorouracil have low gene expression levels of dihydropyrimidine dehydrogenase, thymidylate synthase, and thymidine phosphorylase. Clin Cancer Res 2000;6:1322–7.

48. Kubota T, Watanabe M, Otani Y, Kitajima M, Fukushiuma M. Different pathways of 5-fluorouracil metabolism after continuous venous or bolus injection in patients with colon carcinoma: possible predictive value of thymidylate synthetase mRNA and ribonucleotide reductase for 5-fluorouracil sensitivity. Anticancer Res 2002;22:3537–40.

49. Steg A, Wenquan W, Blanquicett C, et al. Multiple gene expression analyses in paraffin-embedded tissues by Taqman low density array: application to Hedgehog and Wnt pathway analysis in ovarian endometrioid adenocarcinoma. J Mol Diagn. In press 2005.

50. Antoniades J, Brady LW, Lightfoot DA. Lymphangiographic demonstration of the abscopal effect in patients with malignant lymphomas. Int J Radiat Oncol Biol Phys 1977;2:141–7.